CONTRIBUTION AND RESPONSE FUNCTIONS FOR Ca II LINES IN DIFFERENT ATMOSPHERIC MODELS

S. A. GRIGORYEVA, I. P. TUROVA, and R. B. TEPLITSKAYA

SibIZMIR, Irkutsk 33, 664033 U.S.S.R.

(Received 2 October, 1990; in revised form 8 February, 1991)

Abstract. We have calculated profiles of five Ca II lines using three models of the solar atmosphere with different mean temperature gradients in the chromosphere. Contribution functions and response functions to temperature and velocity variations for the line centers and for the K_2 and H_2 emission peaks were found. Disturbances were specified locally at each point of the chromosphere, but for temperature disturbances the other thermodynamical parameter distributions were redetermined. Effective heights of the contribution and response functions, and also the width of the layer reacting to disturbances, depend substantially on the line strength and on the temperature gradient. Contribution curves and response functions to velocity variations differ drastically in form but, in spite of this, their centers of gravity and widths have a similar behaviour. The response function to temperature variations differs from the former two in all its characteristics.

1. Introduction

When using spectral lines as probes of dynamic processes in the solar atmosphere, it is important to know the response function to various perturbations such as disturbances of velocity, temperature, magnetic field, etc., rather than the 'height of line formation' (Beckers and Milkey, 1975). Analytic expressions are known, which are useful for determining the radiation intensity response to a disturbance. Their merit involves saving computer time. On the other hand, when deriving them, simplifying (sometimes, rather restrictive) assumptions are used (see, for example, Gouttebroze, 1983). The influence of the assumptions upon the final results is usually checked by an 'exact' method, i.e., through direct numerical calculations of line profiles for local changes in some parameters.

Response and contribution functions in any known formulations suffer from one common disadvantage, namely they describe in a too simplified manner the process of spectral line formation in a dynamic medium. A self-consistent treatment of atmospheric hydrodynamics and of the radiation transfer problem is significantly more fruitful (e.g., Gouttebroze and Leibacher, 1980). However, the above authors also found it appropriate to use the conceptions of the 'contribution' functions and 'origin' functions for predicting phase relations between velocity and brightness fluctuations.

Codes, fast operating even in the absence of LTE, have become the usual practice of spectral investigations (Carlsson, 1986). With these codes, direct calculations can be performed rather economically. It is particularly easy to determine the response functions to a velocity disturbance if only the velocity does not become so high as to change the source function. It is more difficult to evaluate the effect of temperature perturbations on the emergent intensity. Temperature disturbances lead to changes of

Solar Physics **135:** 1–13, 1991.

both the line absorption coefficients and the source function. Besides, each local departure from the temperature structure requires revising the other thermodynamic parameters in the entire atmosphere model. But even this stage, which implies the use of the equations of hydrostatic and ionization equilibrium, nowadays requires only small expenditures of computer time. In particular, one of the 'fast modeling' programs for atmosphere modeling was developed at our Institute (Grigoryeva, Turova, and Teplitskaya, 1989).

On the basis of codes by Carlsson (1986) and by Grigoryeva, Turova, and Teplitskaya (1989), we shall calculate here the response functions to temperature for H, K, and the infrared triplet Ca II lines at the disk center and on the limb. We shall compare them among each other as well as with the response functions to the velocity and with the contribution curves; moreover, we shall examine how they all depend on the chromosphere model.

2. The Calculations

The emerging line intensity is

$$I_\nu = \int_0^\infty S_\nu(h) \exp(-\tau_\nu(h)/\mu)\,\kappa_\nu\,\mathrm{d}h/\mu\,, \tag{1}$$

where S_ν, τ_ν, and κ_ν are the source function, the total optical depth, and the absorption coefficient in frequency ν, respectively; h is geometrical height; and $\mu = \cos\vartheta$. The integrand in (1) is called the contribution function for the line emission, CF (Babij and Rikalyuk, 1981; Gurtovenko and Sheminova, 1983; Gurtovenko, Sarychev, and Sheminova, 1989).

If some parameter influencing κ_ν or S_ν is disturbed in some layer of the atmosphere, this causes in return a change of I_ν. Let us denote the 'unperturbed' and 'perturbed' intensities by I_ν^u and I_ν^p. Following Demidov (1984) we define the response of I_ν to a disturbance as

$$\mathrm{TF}(h) = \frac{I_\nu^u - I_\nu^p}{I_\nu^u}\,, \tag{2}$$

where TF(h) is a function that gives the measure of the variation of I_ν.

Profiles of five Ca II lines were calculated using the code by Carlsson (1986) near the disk center ($\mu = 0.89$) and near the limb ($\mu = 0.11$) for three atmospheric models, in which the height distributions of temperature T and microturbulence velocity V_t were taken from models of the mean quiet Sun VAL C (Vernazza, Avrett, and Loeser, 1981), and models of a sunspot umbra by Avrett (1981) and Staude (1982). Calculations have been done under the following assumptions: (1) a plane-parallel, semi-infinite atmosphere; (2) Ca II ion model – five levels plus continuum; (3) complete redistribution ($S_\nu = S = \text{const.}(\nu)$); and (4) the absorption profile is a Voigt function.

The five continua were all calculated by specifying the emission temperatures T_r. For the VAL C model, the values of T_r are the same as those used by Carlsson (1986), and the values of T_r for both umbra models are taken from Lites and Skumanich (1982), with the exception of level 4^2P, for which we accepted the value of 4600 K, which was obtained through comparison with an exactly calculated transition (Grigoryeva, Turova, and Teplitskaya, 1989). Shine and Linsky's (1974) atomic parameters of Ca II were used.

The VAL C model and the models by Avrett (1981) and Staude (1982) differ by the mean temperature gradients; the model VAL C and that by Avrett (1981) are characterized by extensive chromospheric plateaus, while the Staude's (1982) model belongs to the so-called 'gradient' type models. Later on, we shall use the mean temperature gradient dT/dh in the chromosphere as the main model characteristic. According to Teplitskaya (1988), for the models under consideration, we find the temperature gradients given in Table I.

TABLE I

Temperature gradients

	VAL C	Avrett (1981)	Staude (1982)
dT/dh	2.2 K km^{-1}	3.8 K km^{-1}	5.2 K km^{-1}

We have calculated 'unperturbed' line profiles and corresponding CF functions for each model. Temperature and macroscopic line-of-sight velocity V were taken as the disturbed parameters, and these disturbances were introduced independently of each other. A set of models was constructed, in each of which a disturbance was specified locally, at one point of the atmosphere, while at the other points the behaviour of the chosen parameter remained unchanged. At the ith point $T_i^p = T_i^u + \delta T_i$; and δT_i makes up 10% of T_i^u in the VAL C model and 15% in both umbral models. The different choice of δT is enforced by with numerical problems (convergence of iterations). For all models, the value of Doppler shift δv_i is taken equal to $0.7\Delta v_{Di}$, where Δv_{Di} is the Doppler width at the ith point of the atmosphere.

Values of TF(h) were determined at the center of each line and, for the H and K lines, also in the regions of the H_2 and K_2 emission peaks. Since the values of I_ν in the intensity minima (H_1, K_1) are distorted due to the neglect of partial redistribution, these line portions are discarded.

In the case of a velocity disturbance, the responses in the H_2, K_2 regions were determined separately for the blue and red peaks and were then averaged.

A temperature disturbance at some point of the atmosphere results in density and electron gas pressure changes throughout the entire atmosphere. So, for each disturbed model, these thermodynamical parameters should be recalculated. Generally accepted methods of calculating the models are hardly applicable in this case because of great expenditures of computer time. A simplified algorithm, suggested by Cram and Giampapa (1987), makes the computational process significantly faster. We have developed (Grigoryeva, Turova, and Teplitskaya, 1989) our version of this algorithm: (1) a hydrogen atom is represented by two bound levels plus continuum; this makes it

possible to determine the Menzel departure coefficient b_1 locally at each point of the atmosphere, without solving an unwieldy set of radiation transfer equations in the entire atmosphere (Kneer and Mattig, 1978); (2) the LTE condition is satisfied for all elements which supply free electrons, except for hydrogen; and (3) the atmosphere is in hydrostatic equilibrium.

In the paper by Cram and Giampapa (1987), the electron density n_e is determined from a given temperature structure and from a known chemical composition as a solution of the quadratic equation

$$[C(1 + Y + 2Z)]n_e^2 + [(1 + Y + Z) + (1 + Z) - CZn_T]n_e - \\ - (1 + Z)n_T = 0\,, \tag{3}$$

where n_T is a total particle density, Y is helium abundance, and Z is abundance of metals. The value of C gives the degree of hydrogen ionization

$$C = \frac{n_0}{n_e n_p} = 4.1416 \times 10^{-16} b_1 T^{-3/2} \exp\left(\frac{157896}{T}\right). \tag{4}$$

Here n_0 is the particle density of neutral hydrogen, and n_p is the proton density.

Equation (3) neglects the ionization of metals and the turbulent pressure $P_t = \rho V_t^2/2$ as well as the fact that a part of the hydrogen is bound in H^-, H_2^+, and H_2 molecules. We have modified Equation (3) for more realistic conditions in a relatively cool solar atmosphere. Without changing the form of Equation (3), we write it as a more exact one:

$$C[(1 + Y + Z) + Z']n_e^2 + [(1 + Y + Z)(1 - Cn'_m) + (1 + Z') - \\ - n_T CZ']n_e + (1 + Y + Z)(n_m - n'_m) - n_T(1 + Z') = 0\,, \tag{5}$$

where

$$Z' = \sum_{k=2}^{K} x_k a_k\,, \qquad x_k = \frac{n_k^+}{n_k}$$

is the degree of ionization of the kth element, and a_k is its abundance (the chemical composition is taken over from the HSRA model). The total density of hydrogen molecules, n_m, and the H^- and H_2^+ ion density, n'_m, are calculated using an algorithm described by Mihalas (1967) and improved by Wittmann (1974).

Equation (5) is a transcendental equation for n_e because the electron density is involved in all coefficients of the quadratic form: in terms of Z' (the Saha equation), in terms of

$$n_T = \frac{gm + n_e D}{kT + D}\,,$$

where

$$D = \frac{1/2\bar{\mu} m_H V_t^2}{1 + Y + Z}\,,$$

m is the column mass density, g is gravity, and

$$\mu = \sum_{k=1}^{K} a_k A_k / A_H \sum_{k=1}^{K} a_k$$

is the mean molecular weight, as well as in terms of n_m and n'_m. This equation, with a given value of b_1, is solved by the method of simple iterations, i.e., it is represented as $n_e = \varphi(n_e)$. At any position in the atmosphere the solution converges after 2 to 5 iterations, depending on the adopted initial value of n_e. Then new values of b_1 are sought with the obtained values of n_e, etc. For a two-level hydrogen atom, we have (Kneer and Mattig, 1978):

$$\frac{1}{b_1(\tau_0)} = G[1 + (\sqrt{\varepsilon_0} - 1) \exp(-\sqrt{3\varepsilon_0}\,\tau_0)] . \tag{6}$$

τ_0 is the optical depth at the head of the Lyman continuum,

$$\tau_0 = 6.319 \times 10^{-18} \int_{h_0}^{h_1} n_1(h)\, \mathrm{d}h ,$$

and n_1 is the density of neutral hydrogen atoms in the ground state ($\approx n_0$). The expressions for ε_0 and G contain collisional and radiative rates (see Kneer and Mattig, 1978).

The method described above, which was realized in the 'fast modeling' code, has permitted us to calculate a rather large number of temperature disturbances. The approximate character of the treatment of the ionization equilibrium alters the electron density as compared with that in the case of a more exact solution (a multi-level hydrogen atom, and LTE for carbon, silicon, and for other suppliers of free electrons). Figure 1(a) shows the variation of electron pressure $P_e(m)$ in the original VAL C model and the variation of $P_e(m)$ obtained after using formula (6) and neglecting the departure from LTE for all elements, except hydrogen. Such a difference leads to a disagreement of the calculated line profiles (Figure 1(b)). It is not our intention here to fit the calculated and observed line profiles. Our main purpose is to understand the behaviour of the function TF(h). Since the TF are, by definition, relative quantities and since the same method is applied for all points of the atmosphere, it might be expected that the height variation of TF(h) is close to the response function which would be obtained through a more rigorous approach.

3. Results of the Calculations

In the beginning we shall consider data for the line centers. As an example, Figure 2 gives the contribution functions CF as well as the response functions to temperature, TFT, and to velocity, TFV, for a spectral H_3 feature in all three models (disk center). The contribution functions and the two response functions differ both from each other and between different models. TFV-curves have a particularly complicated shape: they often

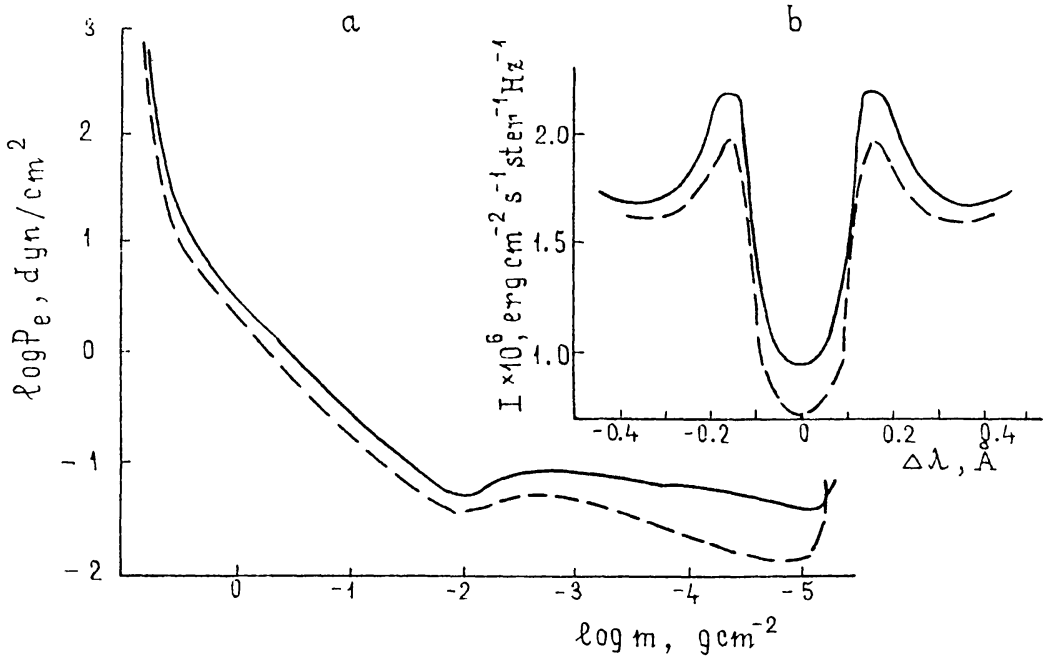

Fig. 1. The influence of an approximate method of calculating the ionization equilibrium on electron pressure P_e and on the H line profile. Solid curve – original VAL C model; dashed curve – approximate model.

show multiple peaks and sometimes even variable signs (see Figure 2, middle panel).

In order to show where and how the atmospheric layers, in which temperature and velocity fluctuations result in changes of emergent intensity are localized, it is appropriate to introduce two parameters. Firstly, these are the centers of gravity of the corresponding curves:

$$\bar{h}(TF_\nu) = \int_0^\infty TF_\nu(h)h\,\mathrm{d}h \Big/ \int_0^\infty TF_\nu(h)\,\mathrm{d}h$$

$$\approx \int_{h_1}^{h_2} TF_\nu(h)h\,\mathrm{d}h \Big/ \int_{h_1}^{h_2} TF_\nu(h)\,\mathrm{d}h\,. \tag{7}$$

The boundary points h_1 and h_2 in each model define the height range, outside which the values of TF are negligibly small. An analogous quantity $\bar{h}$(CF) for the CF function will henceforth be called the effective line formation height. The quantities $\bar{h}$ from (7) will be called the effective heights of response.

The second parameter, d, characterizes the width of the atmospheric region bounded by the CF, TFT, and TFV curves. The values of d were determined on the discrimination level equal to 0.1 from the maximum value on the corresponding curves. In the case of sign-alternating curves, the widths of regions of every sign were summed.

In the case of a very complicated shape of the TFV curves, we have used the quantities

$$h^* = \tfrac{1}{2}d + h_0\,,$$

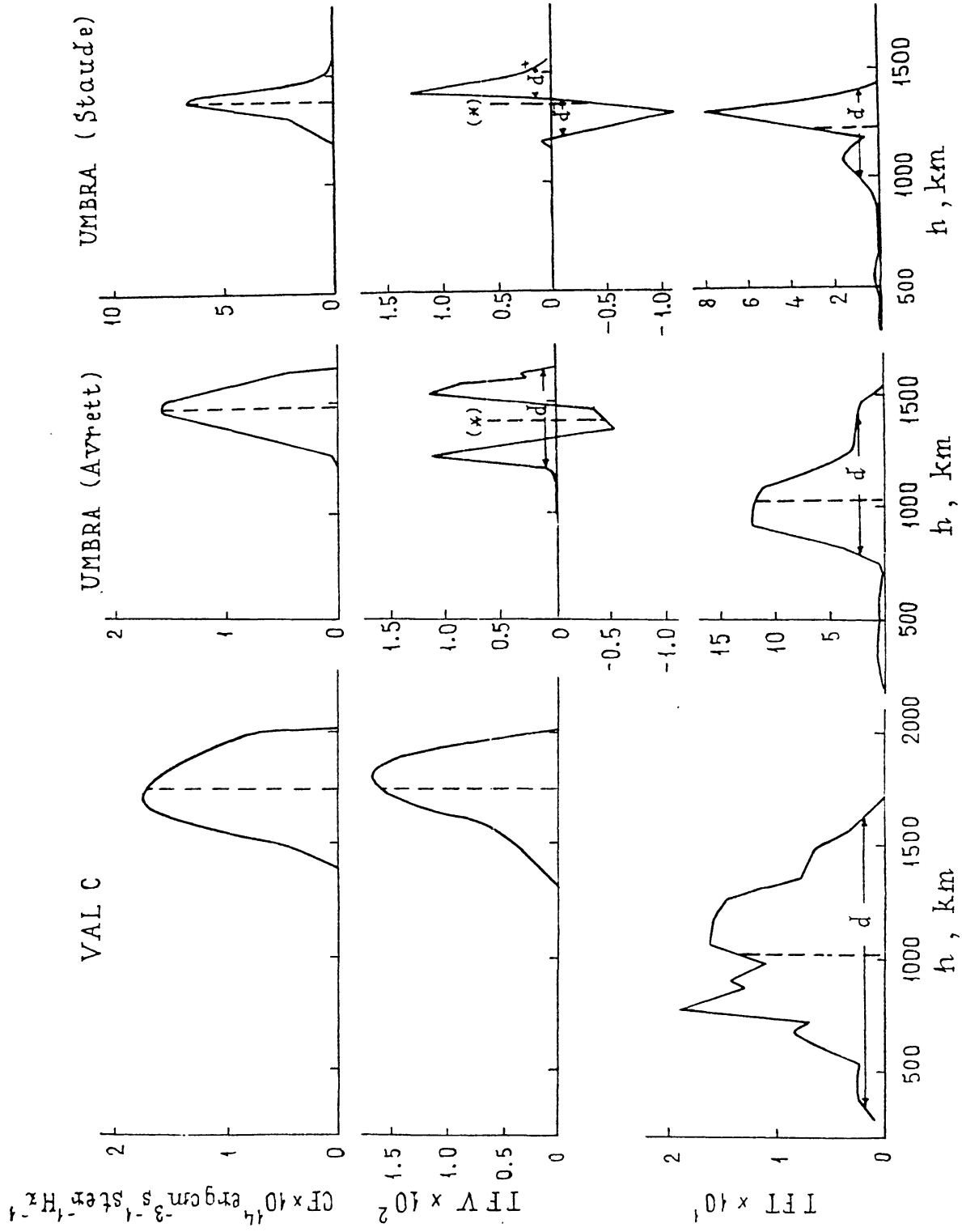

Fig. 2. The contribution (CF) and response functions to velocity (TFV) and temperature (TFT) disturbances for the VAL C model and for two sunspot umbral models. The H_3 line is at disk center. The centers of gravity $\bar{h}$ and the heights h^* (dashed straight lines) are shown; moreover, the methods of measuring the width of the contribution and response d are demonstrated.

instead of centers of gravity, where h_0 is the height of the initial point of the TFV curve taken in accordance with the discrimination level.

In Figure 3 we plot the heights $\bar{h}$ and h^* obtained for the centers of the Ca II lines, against their strength measured by the oscillator strength, f. It is evident that $\bar{h}(h^*)$ are

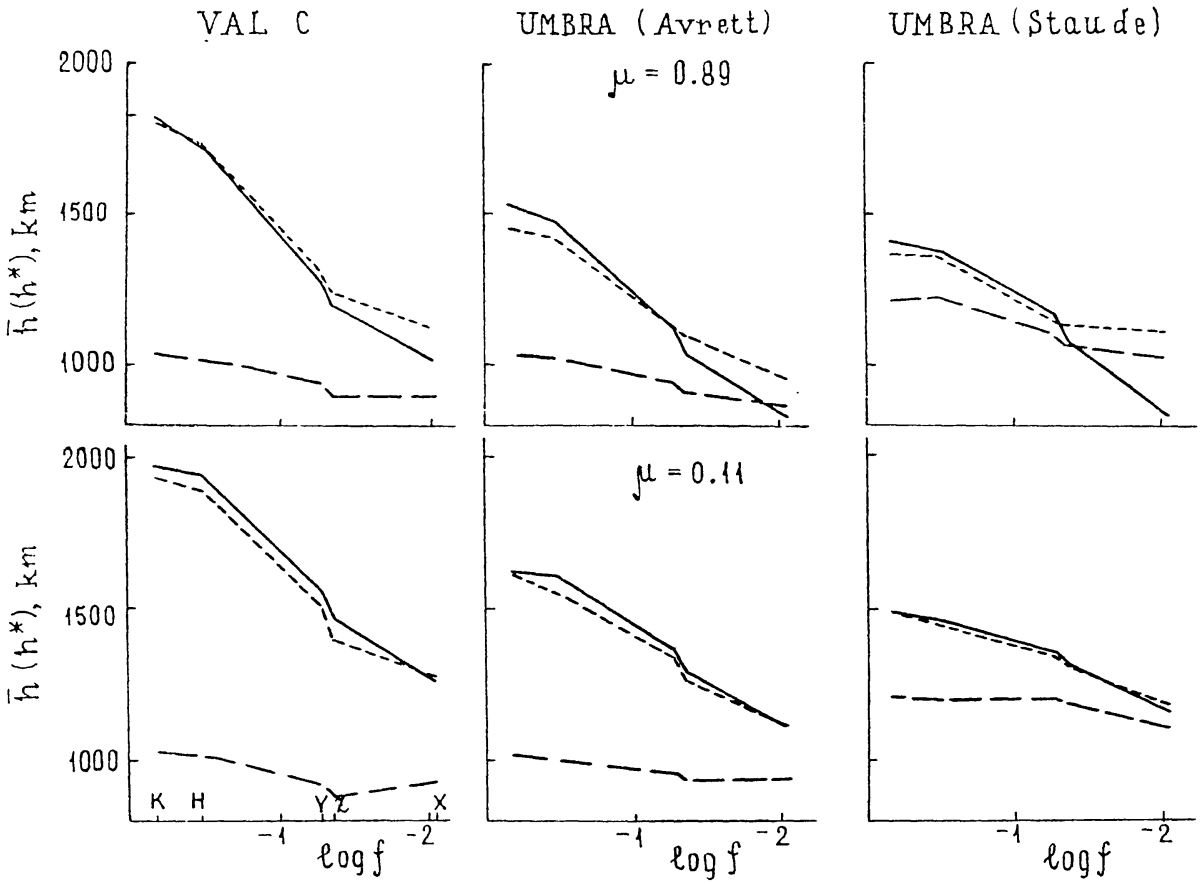

Fig. 3. The dependence of height $\bar{h}$ (or h^*) on the line strength for the centers of the Ca II lines. The solid curve corresponds to CF, the short dashes to TFV, and the long dashes to TFT.

functions of the line strength both at the disk center and near the limb. The effective formation heights and the effective response heights to the velocity show a similar behaviour. Effective heights of response to temperature are much smaller than those for the contribution functions and response functions to the velocity, and they change little with the line strength.

The dependence of effective heights on the line strength is, generally speaking, a well-known fact. Only the weak relationship of effective heights of response to temperature with values of f appears somewhat unusual from this point of view. Of greater interest is the comparison of effective heights for different models. The effective line formation heights and effective heights of response to the velocity proved to depend on the mean temperature gradient, and for the H and K lines they decrease monotonically with increasing dT/dh. Effective heights of response to temperature are, again, distinguished by their behaviour: they increase slightly with increasing dT/dh for all lines

at the disk center and near the limb. For the sake of illustration, Figure 4 gives the dependence of effective heights $\bar{h}(h^*)$ on dT/dh for the K and Z lines at the disk center.

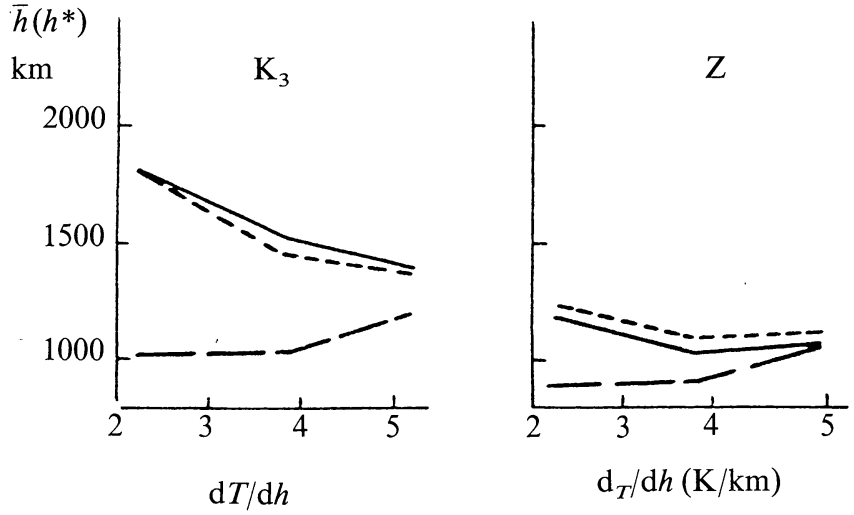

Fig. 4. The dependence of height $\bar{h}$ (or h^*) on the mean temperature gradient in the chromosphere for centers of the K and Z lines (disk center). Symbols are the same as in Figure 3.

Let us consider the second parameter, d. Table II gives the mean ratios of the width of the response functions to temperature and velocity to the width of the contribution function, d(TFT)/d(CF) and d(TFV)/d(CF), respectively. Values of these quantities averaged over lines H and K as well as over the infrared triplet lines, are given here.

TABLE II

Mean ratios d(TFT)/d(CF) and d(TFV)/d(CF)

Model	VAL C		Avrett (1981)		Staude (1982)	
Parameter	T	V	T	V	T	V
			$\mu = 0.89$			
UV	2.65	1.05	2.25	1.3	1.9	1.55
IR	1.95	1.4	0.7	1.15	0.7	1.1
			$\mu = 0.11$			
UV	9.4	1.6	6.3	1.45	2.65	1.15
IR	1.2	1.1	0.9	1.0	1.2	1.05

One can see that the width of the region d(CF), in which the line is formed, nearly coincides with the width of the region in which the response to velocity variation is formed. However, the region, in which the response to a temperature disturbance is generated, is strongly expanded; this refers only to resonance lines and is especially conspicuous near the limb. The effect depends substantially on the model and is most clearly manifested for small mean temperature gradients (the VAL C model).

Finally, it is possible to estimate the size of the region responsible for the formation of the five strong chromospheric Ca II line centers. For this purpose, we have determined the difference of effective heights for the strongest K line and for the weakest X line

$$\Delta(F) = \bar{h}_K(F) - \bar{h}_X(F),$$

where F is one of the functions of response or contribution. The dependence of Δ on dT/dh is shown in Figure 5. One can notice that an increase in the temperature gradient

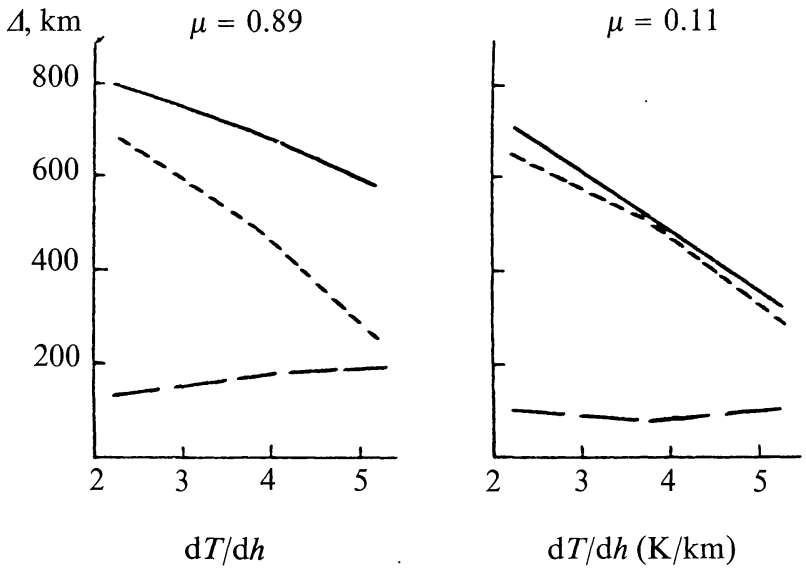

Fig. 5. The dependence of height difference, Δ, on the mean temperature gradient (at disk center and near the limb). Symbols are the same as in Figure 3.

makes the IR and UV line formation layers come closer together, i.e., it leads to a decrease of Δ(CF). The behaviour of Δ(TFV) is similar. However, the total layer of response to temperature remains almost unchanged and even slightly increases with increasing dT/dh.

We have also found the effective heights $\bar{h}(h^*)$ for the K_2 and H_2 emission peaks. The data averaged for both lines are compared with appropriately averaged values for the spectral features of K_3 and H_3 in Table III; it gives the height differences

$$\Delta_{23}(F) = \bar{h}_3(F) - \bar{h}_2(F),$$

TABLE III

Height difference between effective heights of emission peaks and central absorptions, km

μ	0.89			0.11		
Parameter	CF	TFT	TFV	CF	TFT	TFV
VAL C	960	180	462	1150	162	174
Avrett (1981)	535	78	300	640	79	398
Staude (1982)	19	14	175	69	5	132

where $\bar{h}_3(F)$ denotes a value averaged over K_3 and H_3, and $\bar{h}_2(F)$ is averaged over K_2 and H_2.

It is quite evident that the values of Δ_{23} decrease monotonically with increasing temperature gradient (with the only exception of Δ_{23}(TFV) on the limb).

4. Discussion

The above tables and plots clearly show that the response of emergent intensity in the Ca II lines to temperature and velocity disturbances is formed in layers localized in different height intervals, moreover, the height difference depends substantially on atmospheric properties. It is a well-established fact that contribution and response curves and their effective heights do not coincide (e.g., Gouttebroze and Leibacher, 1980; see their Figure 6(a) and our Figure 2, left panel). Therefore, of greater interest is the second statement, namely that this difference cannot be declared *a priori* until the main atmospheric properties of the solar feature under investigation, mainly the mean temperature gradients, are known.

An active region is characterized by a 'chromospheric compression', i.e., by an increase in the mean gradient dT/dh. We have found that the greater is the atmospheric compression, the narrower is the region of contribution to the line intensity (see Figure 2, right panel), the closer are formation layers of strong and moderately-strong lines (Figure 5), and the nearer are the formation levels of emission peaks and central absorptions of the resonance doublet (Table II).

The above facts call for caution when interpeting dynamical processes on the Sun observed in strong spectral lines. This refers especially to the determination of phase relationships from fluctuations of Doppler shifts and intensities in different lines or in the same line at different portions of its profile.

Even if an empirical model of the solar feature under study is known and, consequently, it is possible to determine corresponding effective heights, it is necessary to understand the physical meaning of this notion. It is known that a distinction is made between heights of emergent intensity formation and of line depression formation, and the latter are more informative. However, in central parts of strong lines as treated in this paper, both contribution functions are close to each other (Gurtovenko, Sarychev, and Sheminova, 1989; Sarychev, 1986). Therefore, choosing one of the two contribution functions does not encounter any particular problems in this case.

It is more difficult, however, to understand what is the effective height of response to a velocity disturbance. On some occasions (but not always!) the TFV function has so whimsical a shape that one gets the impression that to some extent the definition of $\bar{h}$ (or h^*) is meaningless. For example, when examining the response function in Figure 2 (umbra, Avrett, 1981), it is scarcely possible to answer the question as to the precise place and sign of the velocity variations needed to cause the observed increase or decrease in intensity at the K line center. To an even greater degree TFV functions are complicated for other line regions, e.g., for the H and K self-reversals. In fact, this result totally agrees with the known conclusion (Athay, 1970) that optically thick lines are a very poor diagnostic tool for studying the line-of-sight velocity field.

Nevertheless, despite this obvious fact, it is surprising that the formally determined $\bar{h}$(TFV) and even h^*(TFV) follow quite definite regularities and, with few exceptions, their behaviour coincides with that of the effective line formation heights, $\bar{h}$(CF). The second parameter, characterizing the response function to the velocity, d(TFV), also behaves in the same manner. Thus, the notion of $\bar{h}$(TFV) and d(TFV) are based on some physical reality.

5. Conclusions

The main conclusions of the present paper are:

(1) The effective formation heights of five strong Ca II line centers and the effective heights of the response to temperature and line-of-sight velocity disturbances depend substantially not only on the line strength but also on the mean temperature gradient dT/dh in the chromosphere.

(2) The contribution function (CF) and the response function (TF) have different shapes. The response functions TFV to velocity disturbances have a particularly complicated shape: a multipeak structure and an inversion of sign are possible. In spite of this, the heights and widths of the curves CF and TFV vary nearly identically, depending on the line strength, dT/dh, and on the location on the solar disk.

(3) The response functions to temperature disturbances TFT differ from CF and TFV not only by their shape but also by their dependence on the line strength and the chromospheric model. TFT depend most weakly on both, and the direction of variations is often opposite to that of CF and TFV.

(4) The layers responsible for the formation of the emission peaks K_2 and H_2 and for their response to temperature and line-of-sight velocity disturbances approach in their position the corresponding layers for the central absorptions of K_3 and H_3 as the mean temperature gradient in the chromosphere increases.

Acknowledgement

We are grateful to Dr E. V. Kononovich for help in the operation of the code by Dr M. Carlsson.

References

Athay, R. G.: 1970, *Solar Phys.* **11**, 347.
Avrett, E. H.: 1981, in L. Cram and J. H. Thomas (eds.), *The Physics of Sunspot.* Sacramento Peak Observatory, p. 235.
Babij, B. T. and Rikalyuk, R. E.: 1981, *Astron. Zh.* **58**, 825.
Beckers, J. M. and Milkey, R. W.: 1975, *Solar Phys.* **43**, 289.
Carlsson, M.: 1986, *Uppsala Astron. Report*, No. 33, 1.
Cram, L. E. and Giampapa, M. S.: 1987, *Astrophys. J.* **323**, 316.
Demidov, M. L.: 1984, *Soln. Dann.* No. 3, 81.
Gouttebroze, P.: 1983, *J. Quant. Spectr. Rad. Trans.* **30**, 193.
Gouttebroze, P. and Leibacher, J. W.: 1980, *Astrophys. J.* **238**, 1134.

Grigoryeva, S. A., Turova, I. P., and Teplitskaya, R. B.: 1989, *Issledovanija po geomagnetismu, aeronomii i fisike Solntsa*, Irkutsk, No. 87, 131.
Gurtovenko, E. A. and Sheminova, V. A.: 1983, *Astron. Zh.* **60**, 982.
Gurtovenko, E. A., Sarychev, A. P., and Sheminova, V. A.: 1989, in R. P. Teplitskaya (ed.), *Solar Magnetic Fields and Corona*, Nauka, Novosibirsk, p. 75.
Kneer, F. and Mattig, W.: 1978, *Astron. Astrophys.* **65**, 17.
Lites, B. W. and Skumanich, A.: 1982, *Astrophys. J. Suppl.* **49**, 293.
Mihalas, D.: 1967, *Methods Comput. Phys.* **7**, 1.
Sarychev, A. P.: 1986, *Astron. Zh.* **63**, 556.
Shine, R. A. and Linsky, J. L.: 1974, *Solar Phys.* **39**, 49.
Staude, J.: 1982, *HHI-STP-Report.* No. 14, Category S, p. 24.
Teplitskaya, R. B.: 1988, *Issledovanija po geomagnetismu, aeronomii i fisike Solntsa*, Irkutsk, No. 83, p. 54.
Vernazza, J. E., Avrett, E. H., and Loeser, R.: 1981, *Astrophys. J. Suppl.* **45**, 635.
Wittmann, A.: 1974, *Solar Phys.* **35**, 11.